applied sciences

MDPI

Article

Mathematical Modeling and Experimental Assessment of Heat Transfer in a Field-Tube Evaporator of a Closed-Loop Two-Phase Thermosyphon

Ivan Martinček *, Milan Malcho, Jozef Jandačka, Ľudmila Nová, Radovan Nosek and Martin Vantúch

Department of Power Engineering, Faculty of Mechanical Engineering, University of Žilina, Univerzitná 8215/1, 010 26 Žilina, Slovakia; milan.malcho@fstroj.uniza.sk (M.M.); jozef.jandacka@fstroj.uniza.sk (J.J.); ludmila.nova@fstroj.uniza.sk (Ľ.N.); radovan.nosek@fstroj.uniza.sk (R.N.); martin.vantuch@fstroj.uniza.sk (M.V.)
* Correspondence: ivan.martincek@fstroj.uniza.sk

Featured Application

The investigated Field-tube heat exchanger integrated into a closed-loop two-phase thermosyphon can be applied as a passive phase-change cooling concept for liquid circuits requiring compact heat removal.

Abstract

This paper presents an experimental and mathematical evaluation of heat transfer in a Field tube heat exchanger integrated into the evaporator section of a closed-loop two-phase thermosyphon. Propylene glycol flowed through 19 parallel Field tubes and transferred heat to distilled water boiling on their outer surfaces. A lumped thermal-resistance model included convective heat transfer in the annular channel, heat conduction through the outer tube wall, nucleate boiling, and secondary heat redistribution between the annulus and the inner return tube. The Hausen, Bergman et al., Gnielinski, and Sieder–Tate formulations were compared for heat transfer in the annulus. Experiments were conducted at propylene glycol volumetric flow rates from 0.0746 to 0.1729 $m^3 \cdot h^{-1}$. The experimental cooling capacity increased from 203.58 to 485.92 W, with a combined relative standard uncertainty of 6.6–8.1%. All models captured the increasing cooling-capacity trend but differed in their absolute predictions. The mean absolute relative deviations were 6.32% for Sieder–Tate, 7.49% for Hausen, 13.89% for Bergman et al., and 17.73% for Gnielinski. The Sieder–Tate correlation therefore provided the lowest deviation for the investigated geometry and operating conditions.

Keywords: Field tube; closed-loop two-phase thermosyphon; heat exchanger; passive phase-change cooling; propylene glycol; annular flow; nucleate boiling; Nusselt number correlation

Check for updates

Academic Editors: Stanislaw Witczak, Krystian Czernek, Daniel Janecki and Zhanjun Cheng

Received: 11 September 2026
Revised: 22 October 2026
Accepted: 23 October 2026
Published: 27 October 2026

Copyright: © 2026 by the authors. Licensee MDPI, Basel, Switzerland. This article is an open access article distributed under the terms and conditions of the Creative Commons Attribution (CC BY) license.

1. Introduction

Closed-loop two-phase thermosyphons allow heat to be removed without mechanically driven circulation of the working fluid within the two-phase circuit itself [1–3]. Heat absorbed in the evaporator section causes the liquid to boil, and the resulting vapor flows into the condenser section, where it transfers latent heat to an external cooling medium. The condensate is then returned to the evaporator section by gravity. The absence of a circulation pump in the two-phase circuit reduces auxiliary energy consumption, the number of active mechanical components, and the risk of operational failure. The utilization of latent heat

of vaporization allows heat transfer even with a relatively small temperature difference between the cooled surface and the saturation temperature of the working fluid. This principle is particularly suitable for geometrically complex or space-constrained equipment in which the creation of conventional cooling channels would be technically challenging.

In the device investigated in this study, heat was extracted from propylene glycol flowing through a bundle of Field tubes. A Field tube consists of two concentric tubes connected at one end [4,5]. Propylene glycol enters the annular channel, changes direction at the end of the tube, and returns through the inner tube. The outer surface of the tube bundle is surrounded by a working fluid, which absorbs heat through nucleate boiling. This configuration provides a compact heat exchanger with a relatively large heat-transfer surface area and single-sided connections for the individual tubes. Heat transfer involves convection from the propylene glycol to the inner wall of the outer tube, heat conduction through the metal wall, and heat transfer to the boiling working fluid. At the same time, secondary heat transfer occurs between the propylene glycol in the annular channel and the return flow in the inner tube. The cooling capacity therefore depends on the flow rate and thermophysical properties of the propylene glycol, the annular geometry, thermal development of the flow, boiling conditions, and internal heat redistribution.

Convective heat transfer in annular channels is commonly characterized using the Reynolds, Prandtl, and Nusselt numbers, while formulations for thermally developing flow additionally involve the Graetz number [5]. The influence of annular geometry on convective heat transfer has also been demonstrated experimentally [6]. In a Field tube configuration, the flow is influenced by the thermal entrance region, the diameter ratio, the change in flow direction at the closed end, and thermal coupling between the annulus and the inner return tube. The choice of the Nusselt number formulation can therefore significantly affect the predicted cooling capacity. Four formulations were compared in this study. The Hausen correlation [7] represents thermally developing laminar flow, the formulation by Bergman et al. [8] represents fully developed heat transfer in a concentric annulus, the Gnielinski correlation [9] accounts for thermal development and the diameter ratio, and the Sieder–Tate correlation [10] accounts for the viscosity difference between the bulk flow and the wall-adjacent region.

Recent studies have examined the thermal performance of two-phase thermosyphons using both experimental and numerical approaches. Ritthong et al. combined experimental measurements with CFD modeling [11], while Sobieraj et al. investigated the heat-transfer performance of a two-phase loop thermosyphon using low-GWP working-fluid mixtures [12]. The effects of working-fluid properties, filling ratio, and two-phase flow behavior were further investigated by Cai et al. [13] and Yin et al. [14].

One potential application of the investigated cooling principle is thermal management of metal hydride hydrogen storage systems, in which heat generated during hydrogen absorption must be effectively removed to maintain favorable reaction conditions [15]. The present study, however, focuses specifically on the heat-transfer behavior of the Field tube evaporator rather than on the experimental investigation of a metal hydride storage system.

The contribution of this work lies in the development and experimental assessment of an integrated thermal-resistance model for a Field tube heat exchanger forming the evaporator section of a closed-loop two-phase thermosyphon. The model simultaneously accounts for heat transfer in the annular channel, heat conduction through the tube walls, nucleate boiling on the external tube surfaces, and internal heat redistribution to the return flow. The objective of this study is to experimentally evaluate the cooling capacity of the Field tube heat exchanger and to compare model predictions obtained using the Hausen [7], Bergman et al. [8], Gnielinski [9], and Sieder–Tate [10] formulations. The comparison is

used to determine which formulation provides the lowest mean absolute relative deviation for the investigated geometry and experimentally verified operating range.

2. Principle of Operation and Experimental Setup

The closed two-phase working fluid circuit operated as a gravity-driven thermosyphon without the use of a circulation pump. The auxiliary propylene glycol circuit was driven by a pump and served to supply heat to the evaporator section. In the evaporator section, the working fluid absorbed heat from the propylene glycol and evaporated. The resulting vapor flowed into the condenser, where it transferred latent heat to an external cooling medium. The condensate then returned to the evaporator section by gravity. The basic principle of the system is illustrated in Figure 1.

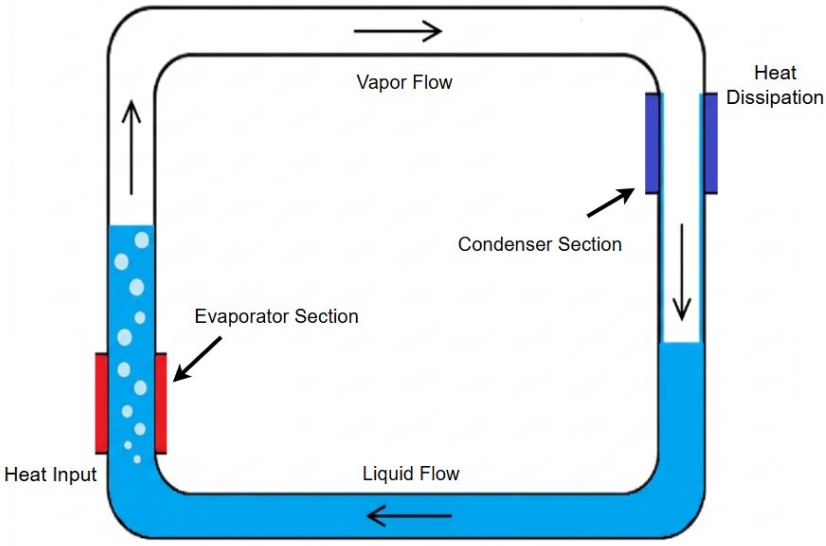


Figure 1. Operating principle of a closed-loop two-phase thermosyphon.

In the configuration analyzed, the evaporator section consisted of a Field tube heat exchanger immersed in the working fluid, distilled water. Heat was extracted from the propylene glycol flowing inside the Field tubes and transferred through their walls to the working fluid, which boiled on the outer surfaces of the tubes. The Field tube system was integrated into the evaporator section of the two-phase circuit. Its structural configuration is shown in Figure 2.

The heat exchanger consisted of 19 Field tubes arranged in five rows containing three, four, five, four, and three tubes, respectively. The horizontal center-to-center spacing between adjacent tubes was 48 mm, and the evaporator vessel had an internal diameter of 250 mm. Each Field tube consisted of an outer tube and an inner return tube. Propylene glycol entered the annular channel between the two tubes, changed direction at the closed end, and returned through the inner tube back into the liquid circuit.

The outer tube had an outer diameter of 43 mm and an inner diameter of 40 mm. The outer and inner diameters of the return tube were 32 and 29 mm, respectively. The wall thickness of both tubes was 1.5 mm; the active length of each tube was 0.595 m, and the tubes were made of stainless steel. The basic geometric parameters of the heat exchanger are listed in Table 1.

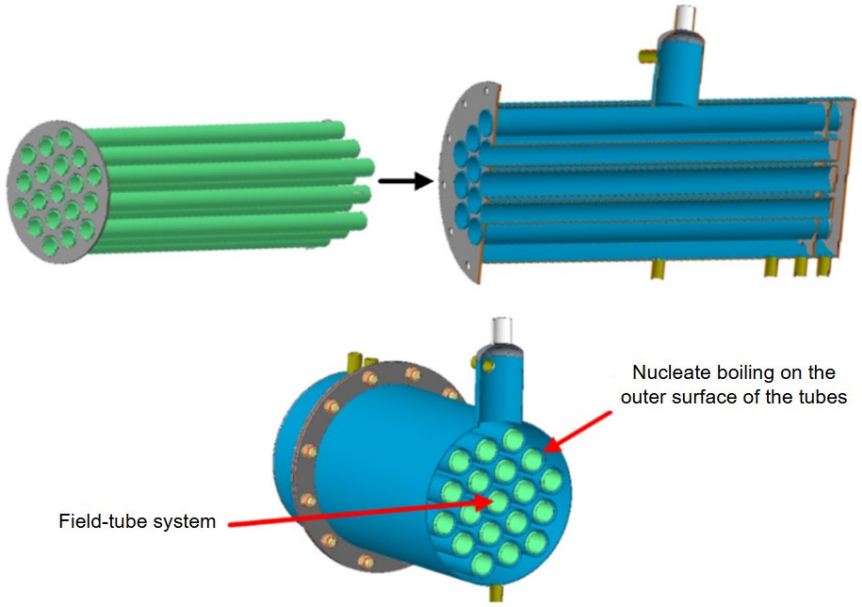


Figure 2. Design of the Field tube system integrated into the evaporator section.

Table 1. Geometric parameters of the Field tube heat exchanger.

	Symbol	Value	Unit
Number of Field tubes	n_t	19	-
Active length of one tube	L_1	0.595	m
Outer diameter of the outer tube	D_{1e}	43	mm
Inner diameter of the outer tube	D_{1i}	40	mm
Outer diameter of the inner tube	D_{2e}	32	mm
Inner diameter of the inner tube	D_{2i}	29	mm
Wall thickness	δ	1.5	mm
Material	-	stainless steel	-

The dimensions of the tube bundle were selected with the aim of creating a compact laboratory platform with a sufficiently large heat transfer area and measurable cooling capacity. The total external heat transfer area of the active section consisting of 19 Field tubes was 1.53 m^2. The selected combination of diameters created an annular channel with a radial width of 4 mm and a hydraulic diameter of 8 mm. This hydraulic diameter was subsequently used as the characteristic dimension in calculating the Reynolds, Graetz, and Nusselt numbers.

The experimental setup consisted of an evaporator section with a Field tube heat exchanger, an external condenser, a closed two-phase working fluid circuit, and an auxiliary propylene glycol circulation circuit. Distilled water was used as the working fluid in the two-phase circuit. Propylene glycol was selected as the auxiliary heat-transfer fluid because its thermophysical properties are well characterized and its pronounced temperature-dependent viscosity provides suitable conditions for evaluating different convective heat-transfer correlations. A schematic of the apparatus, including the locations of the measurement points, is shown in Figure 3.

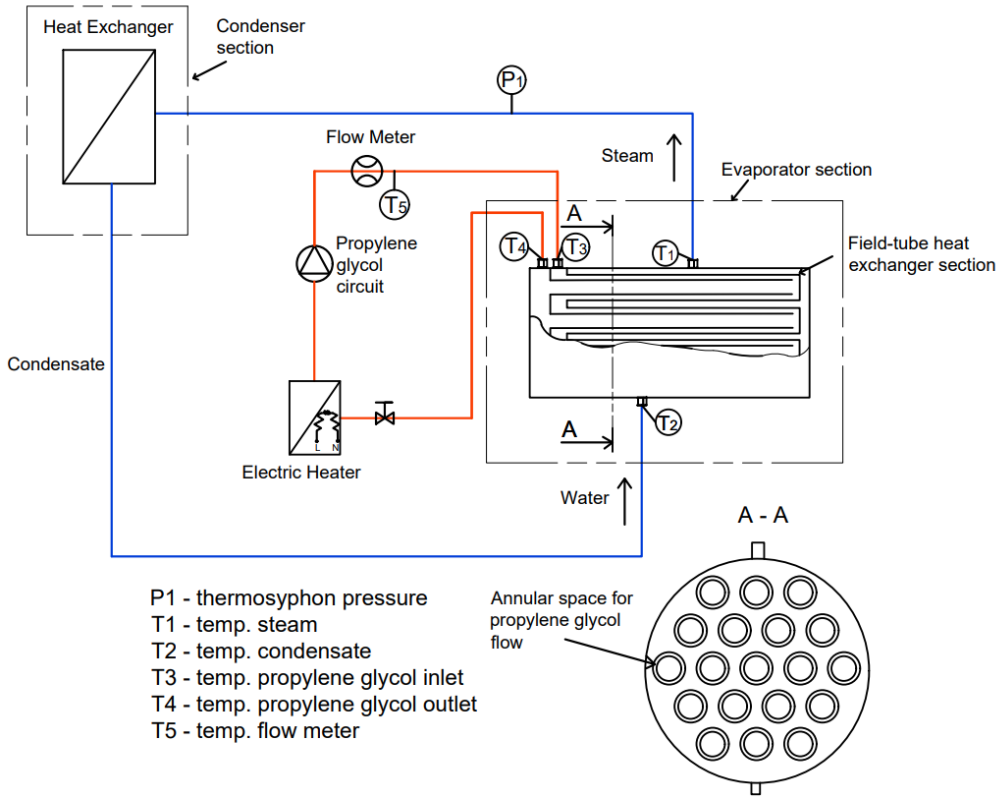


Figure 3. Schematic diagram of the experimental setup comprising a closed-loop two-phase thermosyphon and an auxiliary propylene glycol circuit. The blue and orange lines represent the thermosyphon circuit and the propylene glycol circuit, respectively.

The total volumetric flow rate of propylene glycol was measured using a Yokogawa AXF010G electromagnetic flowmeter (Yokogawa Electric Corporation, Tokyo, Japan) with a 10 mm nominal flow-tube size. The specified standard accuracy was ±0.35% of the reading for flow velocities of 0.3–10 $m \cdot s^{-1}$ and ±1 $mm \cdot s^{-1}$ at lower flow velocities.

The flow-rate signal was continuously recorded by an ALMEMO data acquisition system (Ahlborn Mess- und Regelungstechnik GmbH, Holzkirchen, Germany) at 15 s intervals.

The pressure in the thermosyphon circuit was measured at point P1 using an Ahlborn FD821412A piezoresistive absolute-pressure sensor with a measuring range of 0–10 bar and a specified linearity of ±0.25% of full scale.

The pressure signal was continuously recorded by the central data acquisition system at 15 s intervals. Type K thermocouples were used for temperature measurements at points T1–T5, with a nominal sensitivity of approximately 41 $\mu V \cdot °C^{-1}$.

The thermocouples were calibrated at 120 °C using a Beamex MC6-T temperature calibrator (Beamex Oy Ab, Pietarsaari, Finland).

The calibrator had a specified display uncertainty of ±0.15 °C when using the internal reference. The temperature signals were continuously recorded by the central data acquisition system at 15 s intervals. Thermocouples T3 and T4 recorded the inlet and outlet temperatures of the propylene glycol, respectively, while T5 recorded the temperature at the flowmeter. Thermocouple T1 measured the steam temperature in the evaporator section, and T2 measured the temperature of the condensate returning from the condenser. Before the experiment began, the two-phase circuit was evacuated to an absolute pressure of approximately 6 kPa, primarily to remove non-condensable gases.

Measurements were performed at propylene glycol volumetric flow rates ranging from 0.0746 to 0.1729 $m^3 \cdot h^{-1}$. For each operating point, the system was allowed to stabilize before the steady-state data were evaluated. During the steady-state evaluation intervals, the relative standard deviation of the recorded quantities remained below 1%. The data were recorded at 15 s intervals, and approximately 20–50 consecutive measurements were used to calculate the mean values for each operating point. Each operating point was established once, and no repeated independent experiments were performed for the same operating point. The experimental cooling capacity was then determined from the measured flow rate and the drop in propylene glycol temperature. The obtained operating data were used as reference values for evaluating the mathematical model and comparing the various formulations of the Nusselt number.

3. Mathematical Model

A mathematical model was developed to describe heat transfer in a Field tube heat exchanger constituting the evaporator section of a two-phase system. The model determined the heat transfer from propylene glycol flowing through the Field tubes to the working fluid boiling on the outer surface of the tube bundle.

The calculation was formulated for steady-state conditions and utilized a lumped thermal resistance model for the individual heat transfer branches. It was assumed that the total propylene glycol flow rate was evenly distributed among the 19 Field tubes connected in parallel, that one-dimensional radial heat transfer occurred through the tube walls, and that axial heat conduction and heat losses to the surroundings were negligible.

Uniform flow distribution was assumed because all 19 Field tubes had identical geometry and were connected in parallel. The measured total volumetric flow rate was therefore divided equally among the tubes. Since individual tube flow rates were not measured, possible flow maldistribution was not resolved and may affect the local velocity and heat-transfer coefficient.

The saturation temperature of the working fluid was considered uniform within the tube bundle and was entered into the calculation as a boundary condition for each experimental operating point. These assumptions were considered appropriate for the investigated operating conditions. The steady-state assumption was supported by the several-hour stabilization period before each measurement. The one-dimensional radial heat-transfer approximation was considered reasonable because the tube-wall thickness was small compared with the active tube length. A uniform saturation temperature was assumed because all 19 Field tubes were located within the same evaporator chamber. Residual external heat losses were not resolved separately and remain a limitation of the simplified model. The thermophysical properties of propylene glycol and water were evaluated at the relevant temperatures using published data [16–18].

Heat transfer in a single Field tube consisted of two interconnected branches. In the main branch, heat was transferred at a rate Q from the propylene glycol in the annular channel through the outer tube wall to the circulating working fluid. In the secondary branch, heat was transferred at a rate Q_r from the propylene glycol in the annulus through the wall of the inner tube to the cooler return flow. The secondary branch therefore represented an internal redistribution of energy within the propylene glycol circuit.

In Figure 4 $T_{g,m}$ denotes the bulk mean temperature of propylene glycol in the annular channel, while $T_{g,r}$ denotes the bulk mean temperature of the return flow inside the inner tube. The temperatures $T_{s,1i}$ and $T_{s,1e}$ represent the inner and outer surface temperatures of the outer tube, respectively. The temperatures $T_{s,2i}$ and $T_{s,2e}$ denote the inner and outer surface temperatures of the inner tube, respectively, while T_{sat} is the saturation temperature

of the working fluid. The heat transfer directions considered in the model can therefore be expressed as:

$$T_{g,m} \rightarrow T_{s,1i} \rightarrow T_{s,1e} \rightarrow T_{\text{sat}}, \quad (1)$$

$$T_{g,m} \rightarrow T_{s,2e} \rightarrow T_{s,2i} \rightarrow T_{g,r}. \quad (2)$$

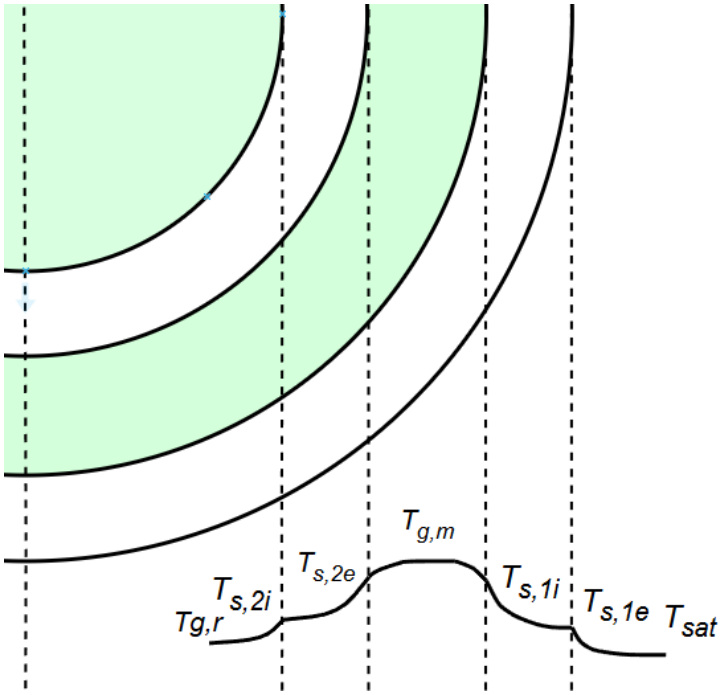


Figure 4. Schematic representation of temperature levels and heat transfer directions in a Field tube during cooling. The light-green regions represent propylene glycol in the annular channel and the inner return tube.

3.1. Heat Transfer in the Annular Channel

The total volumetric flow rate of propylene glycol $\dot{V}_g$ was uniformly distributed among n_t parallel Field tubes. The flow cross-sectional area of the annular channel of a single tube was

$$A_i = \frac{\pi}{4}(D_{1i}^2 - D_{2e}^2), \quad (3)$$

and the mean velocity of propylene glycol in the annular channel was determined as

$$w_i = \frac{\dot{V}_g}{n_t A_i}. \quad (4)$$

The hydraulic diameter of the annular channel was defined as

$$D_h = \frac{4A_i}{P_i}, \quad (5)$$

where the wetted perimeter of the concentric annulus is

$$P_i = \pi(D_{1i} + D_{2e}).$$

For concentric geometry, the hydraulic diameter can therefore be written as

$$D_h = D_{1i} - D_{2e}. \quad (6)$$

For the investigated Field tube $D_h = 8$ mm.

The heat transfer coefficient on the propylene glycol side was calculated from the Nusselt number as

$$\alpha_i = \frac{Nu_i \lambda_g}{D_h}, \tag{7}$$

where λ_g is the thermal conductivity of propylene glycol. The flow in the annular channel was characterized by the Reynolds, Prandtl, and Graetz numbers

$$Re_i = \frac{w_i D_h}{\nu_g}, Pr_i = \frac{\mu_g c_{p,g}}{\lambda_g}, Gz_i = Re_i Pr_i \frac{D_h}{L_1}, \tag{8}$$

where ν_g and μ_g are the kinematic and dynamic viscosities of propylene glycol, respectively, $c_{p,g}$ is its specific heat capacity, and L_1 is the active length of the Field tube. The thermophysical properties of propylene glycol in the annular channel were evaluated at the mean bulk temperature

$$T_{g,m} = \frac{t_{11} + t_{12}}{2}, \tag{9}$$

where t_{11} is the inlet temperature of propylene glycol entering the annular channel and t_{12} is its temperature at the closed end of the Field tube. For correlations incorporating a correction for the liquid properties at the wall, the inner surface temperature of the outer tube was determined from the convective temperature difference

$$T_{s,1i} = T_{g,m} - \frac{Q}{\alpha_i A_{1i}}, \tag{10}$$

where the inner heat transfer area of the outer tubes was

$$A_{1i} = 2\pi r_{1i} L_1 n_t. \tag{11}$$

3.2. Heat Transfer During Boiling of the Working Fluid

Saturated nucleate boiling of water was assumed on the outer surface of the Field tubes. The boiling heat flux was calculated using the Rohsenow [19] correlation

$$q_b'' = \mu_l h_{lv} \left[\frac{g(\rho_l - \rho_v)}{\sigma} \right]^{1/2} \left[\frac{c_{p,l} \Delta T_e}{C_{sf} h_{lv} Pr_l^n} \right]^3, \tag{12}$$

where μ_l is the dynamic viscosity of the liquid phase, h_{lv} is the latent heat of vaporization, ρ_l and ρ_v are the densities of the liquid and vapor phases, respectively, g is the gravitational acceleration, σ is the surface tension, $c_{p,l}$ is the specific heat capacity of the liquid, and Pr_l is its Prandtl number.

The coefficient C_{sf} in the Rohsenow [19] correlation is an empirical parameter that depends on the specific combination of the working fluid and surface, including its surface treatment and operating conditions. Published values for water and stainless-steel surfaces vary depending on the specific surface condition [20]; therefore, a single literature value cannot be directly transferred to a different boiling geometry. In the model $C_{sf} = 0.004$ was used as a single effective parameter representing the boiling side. This value was set consistently for the comparison of the individual Nusselt number correlations and was not subsequently adjusted for individual experimental points or model variants. All correlations considered were therefore evaluated using the same boiling-side description. For water, the exponent $n = 1$.

$$C_{sf} = 0.004, \quad n = 1. \tag{13}$$

The surface superheat was defined as the difference between the outer surface temperature of the tube and the saturation temperature of the working fluid

$$\Delta T_e = T_{s,1e} - T_{\text{sat}}. \tag{14}$$

The heat transfer coefficient during boiling was then determined as

$$\alpha_b = \frac{q''_b}{\Delta T_e}. \tag{15}$$

The total outer surface area of the tube bundle exposed to boiling was

$$A_b = 2\pi r_{1e} L_1 n_t, \tag{16}$$

where r_{1e} is the outer radius of the outer tube. The outer surface temperature was related to the transferred thermal power by

$$T_{s,1e} = T_{\text{sat}} + \frac{Q}{\alpha_b A_b}. \tag{17}$$

The thermophysical properties of water entering the Rohsenow [19] correlation were evaluated at the saturation temperature for each operating point.

3.3. Secondary Heat Transfer to the Inner Tube

After passing through the annular channel, the propylene glycol turned at the closed end of the Field tube and entered the inner return tube. Temperature continuity at the location of the flow reversal was expressed as

$$t_{21} = t_{12}, \tag{18}$$

The temperature t_{12} at the closed end of the Field tube was not measured directly. In the model, it was treated as an unknown variable determined from the simultaneous solution of the energy balances for the annular channel and the inner return branch. Owing to flow continuity, this temperature subsequently represented the inlet temperature t_{21} of the propylene glycol entering the inner tube.

The flow cross-sectional area of the inner tube was

$$A_r = \frac{\pi D_{2i}^2}{4}, \tag{19}$$

and the mean velocity of the return flow was determined as

$$w_r = \frac{\dot{V}_g}{n_t A_r}. \tag{20}$$

The flow in the inner tube was characterized by the Reynolds, Prandtl, and Graetz numbers

$$Re_r = \frac{w_r D_{2i}}{\nu_g}, Pr_r = \frac{\mu_g c_{p,g}}{\lambda_g}, Gz_r = Re_r Pr_r \frac{D_{2i}}{L_1}. \tag{21}$$

The Hausen [7] correlation was used to calculate the Nusselt number in the inner tube

$$Nu_r = 3.66 + \frac{0.0668 Gz_r}{1 + 0.04 Gz_r^{2/3}}. \tag{22}$$

Unlike the annular channel, the inner return branch has a simple circular geometry. The Hausen [7] correlation was selected because, through the Graetz number, it accounts for the thermal development of the flow along the finite active length of the tube and asymptotically approaches $Nu = 3.66$ as the influence of the entrance region decreases, corresponding to a fully developed temperature profile. The same relation was applied to the inner branch in all model variants; therefore, the comparison between the individual models depended solely on the formulation used to describe heat transfer in the annular channel.

The heat transfer coefficient in the inner tube was determined as

$$\alpha_r = \frac{Nu_r \lambda_g}{D_{2i}}. \tag{23}$$

The thermophysical properties of propylene glycol in the return branch were evaluated at the mean bulk temperature

$$T_{g,r} = \frac{t_{21} + t_{22}}{2}, \tag{24}$$

where t_{22} is the final outlet temperature of propylene glycol from the Field tube.

The total thermal resistance of the secondary branch consisted of the convective resistance on the annular-channel side, the conductive resistance through the wall of the inner tube, and the convective resistance on the return-flow side

$$R_r = \frac{1}{\alpha_i 2\pi r_{2e} L_1 n_t} + \frac{\ln(r_{2e}/r_{2i})}{2\pi \lambda_w L_1 n_t} + \frac{1}{\alpha_r 2\pi r_{2i} L_1 n_t}, \tag{25}$$

where r_{2e} and r_{2i} are the outer and inner radii of the inner tube, respectively, and λ_w is the thermal conductivity of the tube-wall material.

Owing to the counter-current arrangement of the model, the secondary heat transfer rate was determined from the mean difference between the bulk temperatures of the two streams

$$Q_r = \frac{T_{g,m} - T_{g,r}}{R_r}. \tag{26}$$

This formulation accounts for the fact that, at the closed end of the Field tube, the outlet temperature of the annular branch is equal to the inlet temperature of the inner return branch.

The energy balances of the annular and inner branches were written as

$$t_{12} = t_{11} - \frac{Q + Q_r}{\dot{m}_g c_{p,g}}, \tag{27}$$

$$t_{22} = t_{21} + \frac{Q_r}{\dot{m}_g c_{p,g}}, \tag{28}$$

where $\dot{m}_g$ is the total mass flow rate of propylene glycol through the tube bundle. By substituting the condition $t_{21} = t_{12}$ the overall energy balance of the Field tube can be expressed as

$$t_{22} = t_{11} - \frac{Q}{\dot{m}_g c_{p,g}}. \tag{29}$$

The secondary heat transfer rate Q_r therefore affects the internal temperature relationships in both flow branches, whereas the total decrease in the bulk temperature of the propylene glycol through the entire Field tube system is determined by the main heat transfer rate Q.

3.4. Main Heat Transfer to the Working Fluid

The main heat-transfer branch consisted of the convective resistance on the propylene glycol side in the annular channel, the conductive resistance through the wall of the outer tube, and the boiling-side heat-transfer resistance of the working fluid. The total thermal resistance of the main branch was expressed as

$$R_{\text{main}} = \frac{1}{\alpha_i 2\pi r_{1i} L_1 n_t} + \frac{\ln(r_{1e}/r_{1i})}{2\pi\lambda_w L_1 n_t} + \frac{1}{\alpha_b 2\pi r_{1e} L_1 n_t}. \tag{30}$$

The main cooling capacity transferred from the propylene glycol to the boiling working fluid was determined from the mean bulk temperature of the propylene glycol and the saturation temperature of the working fluid

$$Q = \frac{T_{g,m} - T_{\text{sat}}}{R_{\text{main}}}. \tag{31}$$

The value Q represents the heat transfer rate removed from the propylene glycol circuit by boiling of the working fluid on the outer surface of the Field tubes. Owing to the nonlinear relationship between Q, the surface temperature, the surface superheat, and the boiling heat transfer coefficient, each operating point was evaluated iteratively until convergence of the calculated quantities was achieved. The mathematical model and iterative calculations were performed using Microsoft Excel for Microsoft 365 (Version 2607, Microsoft Corporation, Redmond, WA, USA).

3.5. Formulation of the Nusselt Number in the Annular Channel

Within the common thermal-resistance framework, four candidate formulations were compared, representing different idealized descriptions of heat transfer on the annular-channel side. In all model variants, the geometric parameters, inlet and boundary conditions, thermophysical properties, boiling model, and description of the secondary heat-transfer branch remained unchanged. The variants differed only in the formulation of the Nusselt number Nu_i, and consequently in the value of the heat transfer coefficient α_i according to Equation (7). This arrangement enabled the influence of the selected description of convective heat transfer in the annular channel on the predicted cooling capacity to be evaluated independently. The annular flow was not assumed to be thermally fully developed in all model variants. Thermal entrance effects are included in the Hausen, Gnielinski, and Sieder–Tate formulations, whereas the Bergman et al. formulation represents the fully developed limiting case.

3.5.1. Hausen Correlation

The Hausen [7] correlation represented the thermal development of the flow through the Graetz number

$$Nu_{\text{H}} = 3.66 + \frac{0.0668 Gz_i}{1 + 0.04 Gz_i^{2/3}}. \tag{32}$$

The Hausen [7] formulation was originally derived for thermally developing laminar flow in a circular tube. For its application to the annular channel, the tube diameter was

replaced by the hydraulic diameter D_h. This formulation therefore provided a reference description of the effect of the thermal entrance region without explicitly accounting for the diameter ratio of the annulus.

3.5.2. Formulation According to Bergman et al.

The formulation according to Bergman et al. [8] represented fully developed heat transfer in a concentric annulus under a constant wall heat flux. For the geometric ratio

$$\frac{D_{2e}}{D_{1i}} = 0.80$$

the following value was used

$$Nu_B = 5.24. \tag{33}$$

The value $Nu_B = 5.24$ represents an idealized fully developed condition under a constant wall heat flux.

3.5.3. Gnielinski Correlation

The Gnielinski [9] correlation accounted for both the thermal development of the flow and the diameter ratio of the annular channel:

$$Nu_{\mathrm{Gn}} = 3.66 + 1.2\left(\frac{D_{1i}}{D_{2e}}\right)^{0.8} + \frac{0.19\left[1 + 0.14\left(\frac{D_{1i}}{D_{2e}}\right)^{0.5}\right]Gz_i^{0.8}}{1 + 0.117Gz_i^{0.467}}, \frac{D_{1i}}{D_{2e}} = 1.25. \tag{34}$$

The Gnielinski [9] formulation was applied to describe thermally developing laminar flow in a concentric annular channel, explicitly accounting for the diameter ratio D_{1i}/D_{2e} and the thermal development of the flow through the Graetz number.

3.5.4. Sieder–Tate Correlation

The Sieder–Tate [10] correlation was used to account for differences between the thermophysical properties of propylene glycol in the bulk flow and those in the vicinity of the heat-transfer surface

$$Nu_{\mathrm{ST}} = 1.86Gz_i^{1/3}\left(\frac{\mu_g}{\mu_s}\right)^{0.14}, \tag{35}$$

The Sieder–Tate [10] formulation was originally derived for thermally developing laminar flow in a circular tube. For its application to the annular channel, the hydraulic diameter D_h was used as the characteristic dimension. The correction term $\left(\mu_g/\mu_s\right)^{0.14}$ accounts for the difference in the dynamic viscosity of the liquid between the bulk flow and the region adjacent to the heat-transfer surface, where μ_g is the dynamic viscosity of propylene glycol evaluated at the mean bulk temperature $T_{g,m}$ and μ_s is the dynamic viscosity evaluated at the inner surface temperature of the outer tube $T_{s,1i}$.

The output of each model variant was the predicted cooling capacity evaluated under identical experimental and operating conditions. This enabled the influence of the Nusselt number formulation in the annular channel on the predicted heat transfer through the heat-exchanger tube wall to be assessed independently.

4. Results

The reference experimental cooling capacity was determined from the calorimetric balance of the propylene glycol between the inlet and outlet measurement locations

$$Q_{\text{exp}} = \frac{\dot{V}_g}{3600}\rho_g(T_m)c_{p,g}(T_m)\left(t_{g,\text{in}} - t_{g,\text{out}}\right), \tag{36}$$

where $\dot{V}_g$ is the volumetric flow rate of propylene glycol, ρ_g is its density, $c_{p,g}$ is its specific heat capacity, and $t_{g,\text{in}}$ and $t_{g,\text{out}}$ are the inlet and outlet temperatures, respectively. For each operating point, the density and specific heat capacity were evaluated at the mean bulk temperature

$$T_m = \frac{t_{g,\text{in}} + t_{g,\text{out}}}{2}. \tag{37}$$

A separate energy balance on the external condenser side could not be established because the cooling-water flow rate was not measured during the experiments. Therefore, the reference experimental cooling capacity used for comparison with the mathematical model was based on the calorimetric balance on the propylene glycol side. The reported experimental cooling capacity was determined directly from the calorimetric balance on the propylene-glycol side and therefore does not require measurement of the condenser cooling-water flow rate. The condenser-side balance would provide an independent verification of the overall system energy balance. Consequently, possible system heat losses or vapor superheating could not be separately quantified from the available measurements.

The uncertainty of the experimental cooling capacity was evaluated from the uncertainties associated with the volumetric flow rate and the inlet and outlet temperatures of the propylene glycol [21]. The temperature dependence of the density and specific heat capacity was incorporated into the corresponding sensitivity coefficients. The combined standard uncertainty was then calculated as

$$u_Q = \sqrt{\left(\frac{\partial Q}{\partial \dot{V}_g}u_{\dot{V}_g}\right)^2 + \left(\frac{\partial Q}{\partial t_{g,\text{in}}}u_{t_{g,\text{in}}}\right)^2 + \left(\frac{\partial Q}{\partial t_{g,\text{out}}}u_{t_{g,\text{out}}}\right)^2}. \tag{38}$$

For the calibrated K-type thermocouples, a standard uncertainty of $u_t = 0.2$ K was used, while the relative standard uncertainty of the electromagnetic flow meter was $u_{\dot{V}_g}/\dot{V}_g = 0.5\%$. The combined relative standard uncertainty of the experimental cooling capacity ranged from 6.6% to 8.1% over the investigated operating range. The corresponding absolute uncertainty values for the individual experimental points were 16.48; 21.78; 27.81; 32.95 and 38.25 W.

The experimental cooling capacity increased with increasing volumetric flow rate of propylene glycol, from 203.58 W at a flow rate of 0.0746 $m^3\,h^{-1}$ to 485.92 W at 0.1729 $m^3\,h^{-1}$.

For each experimental operating point, the predicted cooling capacity was compared with the value determined from the calorimetric balance of the propylene glycol. The relative deviation of the model prediction from the experimental value was calculated as

$$\varepsilon = \frac{Q_{\text{model}} - Q_{\text{exp}}}{Q_{\text{exp}}} \cdot 100. \tag{39}$$

The model results were evaluated at five experimental flow rates, and the comparison with the corresponding experimental cooling capacities is presented in Figure 5.

All compared formulations captured the increasing trend of the cooling capacity; however, they differed in their absolute predictions. The Gnielinski [9] correlation provided the highest values over the entire investigated range and systematically overpredicted the experimental cooling capacity. The mean absolute relative deviation was 17.73%.

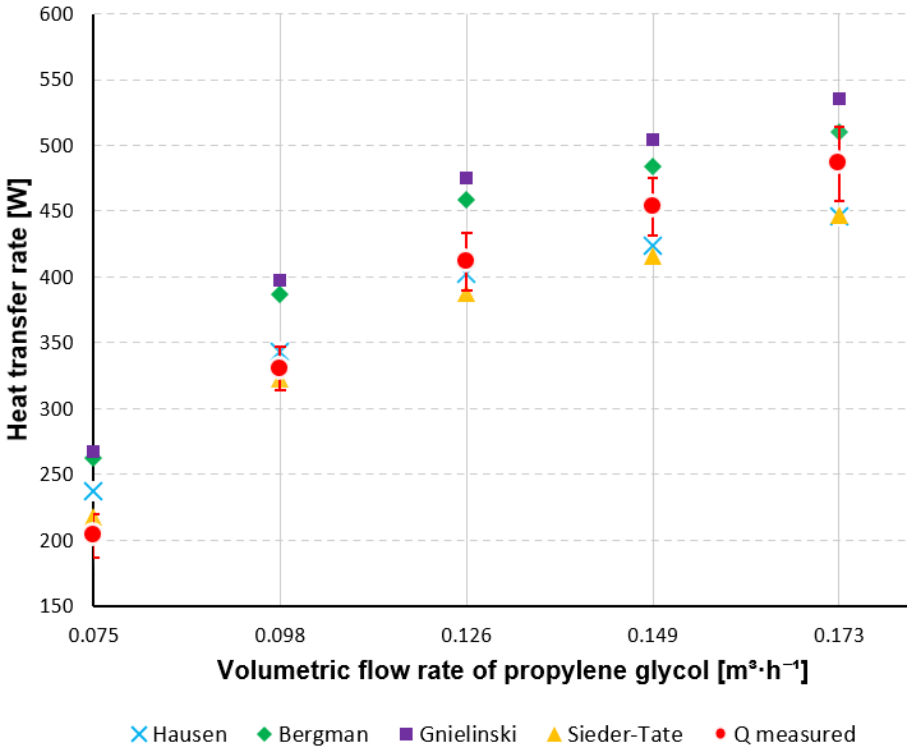


Figure 5. Comparison of the experimental cooling capacity with the results of the mathematical model using the Hausen, Bergman, Gnielinski, and Sieder–Tate correlations. The error bars represent the combined standard uncertainty of the experimental cooling capacity.

The formulation according to Bergman et al. [8] exhibited a similar behavior, although its deviations were lower than those obtained with the Gnielinski [9] correlation. The mean absolute relative deviation was 13.89%. The higher predicted cooling capacities resulted from the higher Nusselt number and, consequently, the lower modeled convective thermal resistance in the annular channel.

The Hausen correlation provided substantially better agreement with the experimental data. At the lowest flow rate, it overpredicted the cooling capacity, whereas at higher flow rates it slightly underpredicted the experimental values. The mean absolute relative deviation was 7.49%.

The lowest mean absolute relative deviation within the analyzed set of experimental points was obtained using the Sieder–Tate [10] correlation. The relative deviation ranged from +7.18% at the lowest flow rate to −8.24% at a flow rate of 0.1489 $m^3\ h^{-1}$. The mean absolute relative deviation calculated from all five experimental points was 6.32%. The corresponding model results obtained using this correlation are summarized in Table 2.

Table 2. Comparison of the experimental and modeled cooling capacities using the Sieder–Tate correlation.

Flow Rate [$m^3\ h^{-1}$]	Q_{exp} [W]	Q_{model} [W]	Deviation [%]
0.0746	203.58	218.20	+7.18
0.0984	330.17	322.50	−2.32
0.1256	411.76	387.63	−5.86
0.1489	453.31	415.95	−8.24
0.1729	485.92	446.98	−8.01

The predicted cooling capacities and relative deviations for all four correlations at the five experimental operating points are provided in Appendix A.

For the Sieder–Tate [10] model, the absolute difference between the predicted and experimental cooling capacities was smaller than the combined standard uncertainty of the experimental cooling capacity at the first three operating points. At the two highest flow rates, the model deviation exceeded this uncertainty, only marginally at the highest flow rate. Among the compared formulations, the Sieder–Tate [10] correlation provided the lowest mean absolute relative deviation.

5. Discussion

The lower deviation obtained with the Sieder–Tate [10] correlation is likely related to the viscosity correction based on the ratio of the dynamic viscosity evaluated at the mean bulk temperature of the propylene glycol to that evaluated at the wall temperature. Given the pronounced temperature dependence of propylene glycol viscosity, this correction partially accounts for the difference between the conditions in the bulk flow and those in the vicinity of the heat-transfer surface.

The experimentally obtained cooling capacity of 203.58–485.92 W provides a reference range for evaluating the heat-removal capability of the proposed Field tube thermosyphon concept. In metal hydride reactors, such data can support the preliminary matching of the cooling system to the expected reaction heat load and can assist in the thermal design and scaling of the heat-removal system [15].

The experimental uncertainty represents the uncertainty of the measured cooling capacity and does not include model-form uncertainty. Therefore, the model–experiment deviation may exceed the experimental uncertainty. The Bergman et al. and Gnielinski formulations predicted higher Nusselt numbers and consequently lower annular-side thermal resistance, resulting in higher predicted cooling capacities. The mathematical model assumed a uniform distribution of the total propylene glycol flow rate among the 19 Field tubes connected in parallel. The saturation temperature of the working fluid was assumed to be uniform throughout the tube bundle, and axial heat conduction through the tube walls was neglected.

Secondary heat transfer between the propylene glycol flowing in the annular channel and the return flow in the inner tube was evaluated using the mean bulk temperatures of both streams. The model therefore describes the overall redistribution of heat between the two branches rather than the local evolution of the temperature field along the active length of the Field tube.

$C_{sf} = 0.004$ was treated as an assumed effective boiling-side parameter and was kept unchanged for all operating points and all model variants. Its value was not independently identified for the actual tube surface; therefore, the absolute model prediction remains dependent on this assumption. However, the same C_{sf} value, boiling model, geometry, and experimentally determined boundary conditions were used in all compared model variants. Therefore, differences between the results of the individual variants arise from the selected Nusselt-number formulation in the annular channel. The comparison results are valid for the investigated geometry, the propylene glycol used, and the experimentally verified range of volumetric flow rates from 0.0746 to 0.1729 $m^3 \cdot h^{-1}$. Application of the model to different geometries, working fluids, or flow regimes requires further experimental verification.

6. Conclusions

This study experimentally and mathematically analyzed heat transfer in a Field tube heat exchanger forming the evaporator section of a closed-loop two-phase thermosyphon. Propylene glycol flowing through the Field tubes transferred heat to water boiling on the

outer surfaces of the tube bundle. The mathematical model included convective heat transfer in the annular channel, heat conduction through the outer tube wall, nucleate boiling of the working fluid, and secondary heat redistribution between the annulus and the inner return tube.

The experimental cooling capacity increased from 203.58 to 485.92 W, as the volumetric flow rate of propylene glycol was increased from 0.0746 to 0.1729 $m^3 \cdot h^{-1}$. All Nusselt number formulations compared showed an increasing trend in cooling capacity but differed significantly in their absolute predictions.

Among the evaluated formulations, the Sieder–Tate correlation provided the best overall agreement with the experimental data, with a mean absolute relative deviation of 6.32%. The Hausen correlation reached 7.49%, the formulation by Bergman et al. 13.89%, and the Gnielinski correlation 17.73%. For the first three experimental data points, the absolute difference between the model and experimental cooling capacities was smaller than the combined standard uncertainty of the experimental cooling capacity. At the two highest flow rates, the model deviation slightly exceeded this uncertainty.

Within the framework of the model assumptions, the Sieder–Tate correlation provided the lowest mean absolute relative deviation among all the formulations evaluated. The obtained results provide a basis for further validation of the model under different Field tube geometries, with other working fluids, over a wider range of flow rates, and through the independent experimental determination of the boiling-side heat-transfer parameters.

Author Contributions: Conceptualization, I.M.; methodology, I.M. and M.M.; formal analysis, I.M. and M.M.; investigation, I.M.; validation, I.M., M.M. and R.N.; resources, J.J. and M.V.; data curation, I.M.; writing—original draft preparation, I.M.; writing—review and editing, I.M., M.M., J.J., Ľ.N., R.N. and M.V.; visualization, I.M.; supervision, J.J. and M.M. All authors have read and agreed to the published version of the manuscript.

Funding: This research was funded by the Cultural and Educational Grant Agency (KEGA), grant number 023ŽU-4/2024, project "Regulation and management of heating and ventilation systems", and by the Scientific Grant Agency (VEGA), grant number 1/0680/23.

Data Availability Statement: The data presented in this study are available on request from the corresponding author.

Conflicts of Interest: The authors declare no conflicts of interest. The funders had no role in the design of the study; in the collection, analysis, or interpretation of data; in the writing of the manuscript; or in the decision to publish the results.

Appendix A

Table A1. Comparison of experimental cooling capacity with the predictions obtained using the four Nusselt-number correlations.

Flow Rate [$m^3 \cdot h^{-1}$]	Q_{exp} [W]	Hausen [W]	Dev. [%]	Bergman [W]	Dev. [%]	Gnielinski [W]	Dev. [%]	Sieder–Tate [W]	Dev. [%]
0.0746	203.58	236.98	+16.41	262.75	+29.06	267.60	+31.45	218.20	+7.18
0.0984	330.17	343.43	+4.02	387.10	+17.24	397.58	+20.42	322.50	−2.32
0.1256	411.76	402.68	−2.21	458.54	+11.36	474.98	+15.35	387.63	−5.86
0.1489	453.31	423.30	−6.62	483.91	+6.75	504.47	+11.29	415.95	−8.24
0.1729	485.92	446.09	−8.20	510.37	+5.03	535.13	+10.13	446.98	−8.01

References

1. Jouhara, H.; Reay, D.; McGlen, R.; Kew, P.; McDonough, J. *Heat Pipes: Theory, Design and Applications*, 7th ed.; Butterworth-Heinemann: Amsterdam, The Netherlands, 2023.
2. Birajdar, M.R.; Sewatkar, C.M. Thermal performance analysis of a closed-loop thermosyphon using ethanol and acetone as working fluids. *Heat Transf.* **2025**, *54*, 2901–2911. [CrossRef]
3. Shi, Y.; Zhang, A. Experimental study on the cooling performance of the two-phase loop thermosyphon with square rib in the evaporator. *Heat Transf.* **2025**, *54*, 4953–4961. [CrossRef]
4. Alzoubi, M.A.; Sasmito, A.P. Thermal performance optimization of a bayonet tube heat exchanger. *Appl. Therm. Eng.* **2017**, *111*, 232–247. [CrossRef]
5. Minhas, H.S.; Lock, G.S.H. Numerical analysis of heat transfer in an air-filled bayonet tube under laminar conditions. *Int. J. Heat Mass Transf.* **1996**, *39*, 761–769. [CrossRef]
6. Serrano García, D.; Sánchez-Delgado, S.; Pérez-Álvarez, R.; Acosta-Iborra, A. Experimental determination of the convection heat transfer coefficient in an eccentric annular duct. *Exp. Therm. Fluid Sci.* **2022**, *136*, 110664. [CrossRef]
7. Hausen, H. Darstellung des Wärmeüberganges in Rohren durch verallgemeinerte Potenzbeziehungen. *Z. VDI Beih. Verfahrenstech.* **1943**, *4*, 91–98.
8. Bergman, T.L.; Lavine, A.S.; Incropera, F.P.; DeWitt, D.P. *Fundamentals of Heat and Mass Transfer*, 7th ed.; John Wiley & Sons: Hoboken, NJ, USA, 2011.
9. Gnielinski, V. G2 Heat Transfer in Concentric Annular and Parallel Plate Ducts. In *VDI Heat Atlas*, 2nd ed.; VDI e.V., Ed.; Springer: Berlin/Heidelberg, Germany, 2010; pp. 701–708. [CrossRef]
10. Sieder, E.N.; Tate, G.E. Heat transfer and pressure drop of liquids in tubes. *Ind. Eng. Chem.* **1936**, *28*, 1429–1435. [CrossRef]
11. Ritthong, N.; Thongkom, S.; Sawisit, A.; Duangsa, B.; Ritthong, W. Optimization Design of Closed-Loop Thermosyphons: Experimentation and Computational Fluid Dynamics Modeling. *Energies* **2024**, *17*, 527. [CrossRef]
12. Sobieraj, M.; Ksionek, D.; Kamiński, M.; Karczmarczyk, F. Experimental Investigation of the Two-Phase Loop Thermosyphon Working with Low-GWP Mixtures for Heat Reclaim. *ChemEngineering* **2025**, *9*, 131. [CrossRef]
13. Cai, Y.; Hu, X.; Lu, J.; Li, Y.; Tang, D.; Hu, C. Impact of working fluid properties on heat transfer and flow characteristics of two-phase loop thermosyphon with high filling ratios. *Int. J. Heat Mass Transf.* **2025**, *238*, 126482. [CrossRef]
14. Yin, C.; Wang, K.; Zhou, J.; Tang, D. Visualization Study on Flow Pattern Evolution and Heat Transfer Characteristics of a Two-Phase Loop Thermosyphon Under High Heat Flux with Various Filling Ratios. *Energies* **2026**, *19*, 2674. [CrossRef]
15. Su, J.-W.; Tang, X.-Y.; Bai, X.-S.; Yang, W.-W.; Zhang, J.-F.; Qu, Z.-G. Review on thermal design and thermal management for metal hydride reactors: Current status and future development. *Int. J. Hydrogen Energy* **2025**, *114*, 295–311. [CrossRef]
16. Sun, T.; Teja, A.S. Density, viscosity and thermal conductivity of aqueous solutions of propylene glycol, dipropylene glycol, and tripropylene glycol between 290 K and 460 K. *J. Chem. Eng. Data* **2004**, *49*, 1311–1317. [CrossRef]
17. National Institute of Standards and Technology (NIST). *NIST Chemistry WebBook, SRD 69: Propylene Glycol (CAS 57-55-6)*; National Institute of Standards and Technology: Gaithersburg, MD, USA, 2025. [CrossRef]
18. International Association for the Properties of Water and Steam (IAPWS). *Revised Release on the IAPWS Formulation 1995 for the Thermodynamic Properties of Ordinary Water Substance for General and Scientific Use*; IAPWS R6-95(2018); IAPWS: Erie, CO, USA, 2018.
19. Rohsenow, W.M. A method of correlating heat-transfer data for surface boiling of liquids. *J. Fluids Eng.* **1952**, *74*, 969–975. [CrossRef]
20. Pioro, I.L. Experimental evaluation of constants for the Rohsenow pool boiling correlation. *Int. J. Heat Mass Transf.* **1999**, *42*, 2003–2013. [CrossRef]
21. Moffat, R.J. Describing the uncertainties in experimental results. *Exp. Therm. Fluid Sci.* **1988**, *1*, 3–17. [CrossRef]

Disclaimer/Publisher's Note: The statements, opinions and data contained in all publications are solely those of the individual author(s) and contributor(s) and not of MDPI and/or the editor(s). MDPI and/or the editor(s) disclaim responsibility for any injury to people or property resulting from any ideas, methods, instructions or products referred to in the content.